

In situ energy dispersive x-ray reflectometry to investigate the (RuPc)₂/NO_x interaction process evidenced by ex situ measurements

Amanda Generosi, Barbara Paci,^{a)} Valerio Rossi Albertini, and Paolo Perfetti
*Istituto di Struttura della Materia-Area di Ricerca di Tor Vergata, Via del Fosso del Cavaliere 100,
 00133 Roma, Italy*

Anna M. Paoletti, Gianna Pennesi, and Gentilina Rossi
*Istituto di Struttura della Materia-Area di Ricerca di Montelibretti, Via Salaria Km. 29.5,
 Casella Portale 10 Monterotondo Stazione, I-00016 Roma, Italy*

Ruggero Caminiti
*Dipartimento di Chimica, Università "La Sapienza" di Roma e sezione INFM, Piazzale Aldo Moro 5,
 00185 Roma, Italy*

(Received 31 May 2005; accepted 6 January 2006; published online 16 February 2006)

A systematic energy dispersive x-ray reflectometry study of different ruthenium phthalocyanine (RuPc)₂ thin films was performed in order to investigate their reactivity with the oxidizing NO_x gas. A preliminary *ex situ* analysis, consisting of the comparison between the morphological parameters of different films (before and after the exposure to the gas), was performed. It suggests that a reaction involving two different mechanisms takes place. The following *in situ* (while fluxing the gas) reflectometry analysis confirms this hypothesis, and clarifies the temporal evolution, also revealing that the first mechanism is limited to the film surface, while the second is a bulk diffusion process. © 2006 American Institute of Physics. [DOI: 10.1063/1.2171778]

I. INTRODUCTION

The architectural flexibility and environmental stability of phthalocyanines (Pc), their metalloderivates (MePc), and related compounds make these molecules suitable for a number of technological applications.¹⁻³ Moreover, the electrical properties of the phthalocyanines change upon exposure to gases such as NO₂ or ammonia,⁴⁻⁶ this has led to an interest in developing gas detectors which have Pc derivatives as the chemically sensitive component of chemical/conductometric transduction systems.^{7,8}

Films of different MePc are known to be characterized by different packing and long-range structures,^{9,10} and different interaction mechanisms are expected during the process of gas diffusion into the sensing material. In a previous study,^{11,12} it was demonstrated that the gas diffusion within MePc films occurs at various stages that correlate with morphological changes. It is for this reason that they can be used to monitor the gas sensing process. Moreover, film morphology affects both the adsorption/desorption properties¹³ and the sensor's performances (reversibility, response time, and recovery rates). While much work has been dedicated to the former aspect,¹⁴⁻¹⁶ the latter has not been investigated in depth until now. In the literature,¹⁷ an adsorption/desorption process, coupled with bulk diffusion, has been successfully used to account for NO₂ diffusion into lead phthalocyanine (PbPc₂) thin films. The packing of such molecules, when processed as thin films, is well known⁹ and can be as a stack of single phthalocyanine rings with the metal located in the cavity. However, thin films of (RuPc)₂ are packed in a different way, which may be described as a sandwich,¹⁸ the

layers containing two aromatic rings coordinated by two Ru atoms bound to each other. The kinetics of the interaction is still unclear for such materials.

The aim of the present paper is to study the change in the morphological characteristics (average thickness and roughness) during the exposure of (RuPc)₂ thin films to a mixture of NO_x gas molecules. For this purpose, the energy dispersive x-ray reflectometry (EDXR) technique was used. This allowed the real-time variations of the morphological parameters of films to be followed *in situ*.^{12,19}

II. EXPERIMENT

A. Theory

X-ray reflectometry is a technique that is sensitive to surface and interface morphology at the angstrom resolution and is commonly utilized to probe the properties of surfaces and interfaces of layered samples (films deposited on substrates, multilayers, superlattices, etc.).²⁰

The method utilized here makes use of the optical properties of x-rays, which will be outlined briefly, and is fully reported elsewhere.^{20,21}

In optics, with reference to the film surface, Snell's law can be expressed as $n_1 \cos \theta_1 = n_2 \cos \theta_2$, (θ_1 and n_1 being the incidence angle of the primary beam and the refractive index of the first medium, respectively and θ_2 and n_2 the reflection angle and the refractive index of the second medium, respectively). If the first medium is a vacuum (or air), $n_1 = 1$ and the previous equation, at the critical angle θ_c , takes the form: $\cos \theta_c = n_2$, since when $\theta_1 = \theta_c$, $\theta_2 = 0$.

In the x-ray energy range, the refractive index can be expressed as

^{a)}Electronic mail: barbara.paci@ism.cnr.it; FAX: +39-064993153

$$n = 1 - (\lambda^2/2\pi)\rho r_0 Z^2 + i(\lambda/4\pi)\mu,$$

(λ being the incident wavelength, ρ the material density, r_0 the classical electron radius, Z the atomic number, and μ the linear absorption coefficient, typically 10^{-6} – 10^{-7} that is therefore negligible).

Therefore, total reflection conditions are fulfilled when $\cos \theta_c = 1 - (\lambda^2/2\pi)\rho r_0 Z^2$, which, at the second order of approximation, can be summarized as $\theta_c/\lambda = \text{const}$. Since, in an x-ray scattering process, the scattering parameter q (normalized momentum transfer) can be expressed as $q = 4\pi \sin \theta / \lambda = KE \sin \theta$ and, in grazing incidence conditions, $\sin \theta \approx \theta$, we can rewrite the total reflection condition as $\theta_c/\lambda = q_c$. The q range of interest in a total reflection measurement, i.e., the q range containing the morphological information, is around this critical value of the scattering parameter q_c .

Indeed, the position of the critical edge (q_c) and the slope of the reflectivity profile above q_c are determined by the material density and the surface roughness (variance from the average thickness), respectively. Furthermore, if the sample consists of a thin film deposited on a thick substrate, the signal exhibits oscillations produced by the interference of the two waves reflected at the surface and interface. In this case, the frequency of the oscillations is roughly proportional to the film thickness, while their damping is related to the surface and interface roughness.^{20,21}

Two ways can be used to collect an x-ray reflection pattern, that is, the reflected intensity as a function of q . The q scan can be accomplished either by utilizing a monochromatic beam and carrying out an angular scan (angular dispersive mode adopted in commercial x-ray reflectometers) or using a polychromatic x-ray beam at a fixed angle and carrying out an energy scan (ED mode), no movement being required.^{22,23} The following measurements were performed by using a homemade ED x-ray reflectometer.²⁴

This method was chosen since the advantages of the ED technique over the angular dispersive counterpart, mainly related to the immobility of the experimental setup, are quite remarkable regarding reflectometry measurements on evolving systems.¹² Indeed, the immobility of the experimental setup reduces the systematic errors induced by the angular scan (misalignments and aberrations) and guarantees the reproducibility of the experimental conditions (particularly critical at small angles), when many consecutive measurements have to be performed, as in the present case. This allows *in situ* investigations to be performed with an extremely high degree of confidence. Moreover, in the ED mode, a single spectrum collected at a fixed angle, which covers a range of some 10^{-1} \AA^{-1} , is made of a collection of several hundred points, with the q resolution approaching 10^{-4} \AA^{-1} . A q resolution of this order would hardly be achieved using a conventional laboratory angular dispersive reflectometer. On the other hand, the main drawback of the ED mode, i.e., the decrease in the q resolution due to the uncertainties of both the angle and the energy, does not affect reflectivity measurements since the EDXR pattern of a thin film is characterized by long period oscillations.

B. The EDXR diffractometer

The energy dispersive x-ray reflectometer²³ is provided with two benches, one carrying the x-ray tube, the other the energy-sensitive detector, pivoting around a single central axis. The x-ray optical path is defined by four variable slits mounted on the arms. The arms are moved by two linear actuators driven by step motors and the tangent of the angle is read by two linear encoders. Both the minimum step movement and the resolution of the encoders are $1 \mu\text{m}$, which, in our case, guarantees a reproducible minimum angle increment of 0.004° .

The white incident beam is produced by a standard 2 kW tungsten anode x-ray tube and detection is accomplished by a EG&G high-purity germanium solid-state detector. The detector is connected to a PC via ADCAM hardware and the signal is processed by MAESTRO software, which performs the necessary analog-to-digital conversions. The energy resolution $\Delta E/E$ is ca. 1.5% in the energy range of interest (20–50 keV). Neither a monochromator nor goniometer is required in the energy dispersive mode.

C. Sample deposition

The ruthenium phthalocyanine thin films were obtained by sublimation under vacuum of a $(\text{RuPc})_2$ powder according to the procedures previously reported.⁹ An Edwards Auto 306 vacuum coater with diffusion pumping system, able to reach 10^{-5} – 10^{-6} mbar of pressure, was used to prepare the films on Si $\langle 111 \rangle$ substrates. Growth was monitored by an Edwards FTM5 quartz crystal balance, by measuring the change in its resonance frequency consequent to exposure to the MePc molecule flux during film deposition.

III. RESULTS AND DISCUSSION

A systematic analysis of the NO_x adsorption-desorption cycles on $(\text{RuPc})_2$ thin films of different thickness was performed. The gas sensing films, with a surface area of $\approx 1 \text{ cm}^2$, were placed in an experimental chamber¹¹ and exposed to a gas flux of N_2 containing 50 ppm of NO_x , which corresponds in our setup to a rate of 20 nmol/s. After complete saturation was reached, each film was submitted to a desorption cycle by flushing the systems with pure N_2 gas at 180 nmol/s (900 ppm) for another day and, finally, the sample was left in air (room conditions) and periodically (every month) remeasured (*ex situ* EDXR) to check the morphological stability. A preliminary *ex situ* analysis, consisting of a comparison between the morphological parameters of different films (before and after the exposure to the gas), was performed. As an example, the *ex situ* reflectivity spectra, collected before and after exposure to NO_x for a 103-nm-thick film, are reported in Fig. 1. The shift towards lower q values of the oscillations of the latter spectrum indicates that the film becomes thicker as a consequence of its exposure to the gas.

In order to extract numerical values for the morphological parameters from the EDXR data the spectra need to be analyzed (after normalization to the energy-dependent primary beam), to deduce the initial and final thicknesses and roughnesses of the films. The data were fitted on the basis of

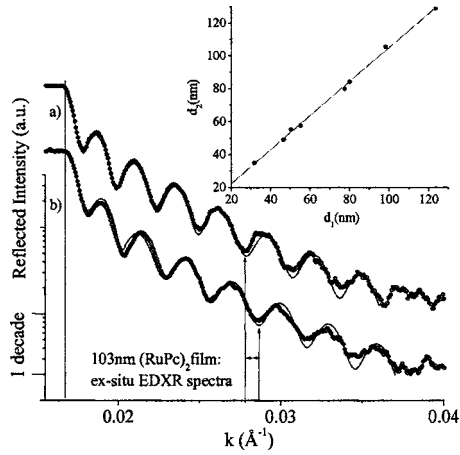


FIG. 1. Reflectivity spectra, collected during the NO_x -film interaction, are plotted as a function of the scattering parameter: (a) 50-nm-thick film and (b) 100-nm-thick film. The fact that oscillations shift towards lower q values indicates that the $(\text{RuPc})_2$ film is swallowing.

the Parratt model,²⁵ which describes the reflection of an x-ray beam by a thin film separated from its substrate by a sharp interface. When the surface and/or the interface are not sharp, the reflected intensity is modified by a roughness terms that play a role similar to the Debye-Waller factor in diffraction patterns. In the present case the substrate is monocrystalline silicon and the roughness of this interface is much smaller than that of the film surface and can therefore be neglected.^{26,27} Therefore, considering only the film surface roughness, the general expression for the reflected intensity is

$$|R|^2 = \{ |R_f|^2 |\exp(-2k_0 k_f \sigma^2)| + |R_r|^2 - 2 \text{Re}[R_f R_r] \times \exp(-2k_0 k_f \sigma^2) \exp(2ik_f d) / 1 + |R_f|^2 |R_r|^2 \times \exp(-2k_0 k_f \sigma^2) - 2 \text{Re}[R_f R_r \exp(-2k_0 k_f \sigma^2) \times \exp(2ik_f d)] \},$$

where $k_0 = q/2$ is the radiation wave number in the air, $R_f = (k_0 - k_f)/(k_0 + k_f)$ is the Fresnel film material reflectivity, $R_r = (k_f - k_s)/(k_f + k_s)$ is the Fresnel substrate material reflectivity,²⁰ d is the average thickness of the film, and σ is the surface roughness.

The quantities k_f and k_s are the radiation wave numbers in the film and in the substrate, which depend greatly on k_0 :²⁰ $k_f = (k_0^2 - 4\pi\rho_f)^{1/2}$ and $k_s = (k_0^2 - 4\pi\rho_s)^{1/2}$.

The *ex situ* EDXR measurements were performed on several films of various nominal thicknesses. As a result, the final thicknesses of the films (d_2) can be plotted versus their initial values (d_1) to get an overview of the swelling process. The most straightforward hypothesis to account for this thickness increase is that the film undergoes a “breathing-like” mechanism as an effect of the gas diffusion process;²⁸ in this case the final d value (d_2) should be proportional to the initial film thickness. However, the experimental points plotted in the insert of Fig. 2 give indication that this hypothesis is not fulfilled in the present case. Indeed, the data follow a linear trend²⁸ that can, at best, fit the relation: $d_2 = d_1 (1.038 \pm 0.021) + (1.68 \pm 1.44)$, namely, a straight line with a

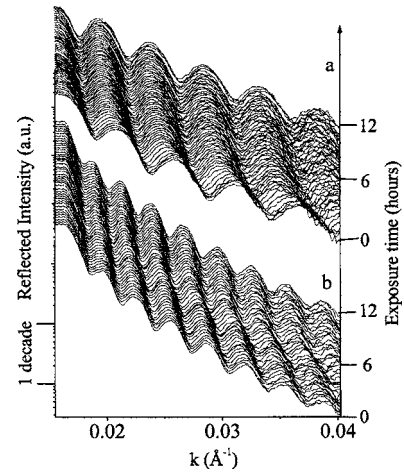


FIG. 2. Reflectivity spectra, collected during the NO_x -film interaction, are plotted as a function of the scattering parameter: (a) 50-nm-thick film and (b) 100-nm-thick film. The fact that oscillations shift towards lower q values indicates that the $(\text{RuPc})_2$ film is swallowing.

unitary slope coefficient, which does not cross the origin of the axes.

This suggests that the film transformation is due to two contributions, the first being a constant increase of about 1.7 nm and is independent of the initial film thickness d_1 , while the second is proportional to d_1 . This observation implies that the swelling process actually involves two distinct mechanisms, each producing one of these two effects. A natural hypothesis is that the constant part is due to a thickness expansion mechanism that does not involve the bulk, but the surface only. Indeed, in this way, it would explain why this contribution does not change in relation to film thickness.

The proportional contribution, instead, is the result of a bulk interaction, whose effect is greater the thicker the film. This kind of single step diffusion mechanism (sigmoidal growth of the d parameter) has already been proven for other metal-phthalocyanine thin films.²⁸ *In situ* EDXR measurements may provide the information needed to validate the former hypothesis. The next step therefore consisted of following the morphological evolution of the film during gas exposure: while the gas was flowing in the test chamber containing the sample. X-ray reflectivity spectra were collected in sequence every 15 min. As discussed in the Experiment section, this *in situ* experimental setup allows the evolution of the film morphology to be monitored with great accuracy,²⁹ preventing errors that may affect the traditional *ex situ* measurements, i.e., the difficulty of repositioning the sample under the x-ray beam, since minimal sample misplacements can produce artifacts in the reflectivity spectrum.¹⁹ Furthermore, in this way, we were able to observe not only the initial and the final states of the films as in *ex situ* measurements, but also the intermediate stages of the transformation following, in this way, the real-time evolution of the morphology. As an example, two sequences of reflectivity spectra are shown in Fig. 2, in the case of two films having nominal thicknesses (measured by a quartz balance) of 50 nm (a) and of 100 nm (b), respectively. Both sequences represent spectra acquired during the first 12 h of exposure

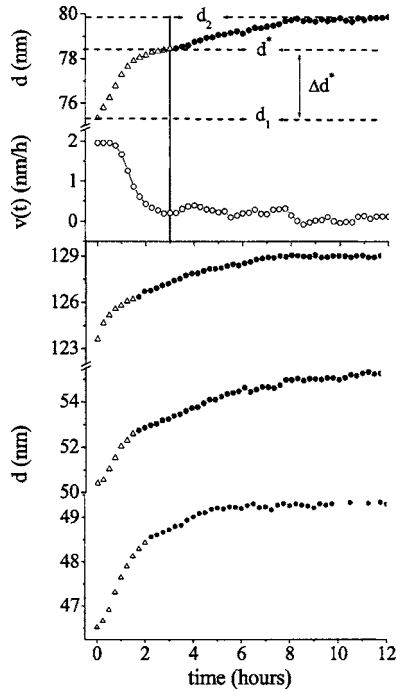


FIG. 3. The kinetic evolution of film thickness during the NO_x -(RuPc) $_2$ interaction as a function of time is shown in the case of four different samples [(a), (c), (d), and (e)]. Different fonts are used to point out the two different reaction stages (triangle, first step; dot, second step), i.e., the thickness crossover value d^* . In (b), the derivative of (a) is represented, to make the crossover value more evident. The symbols used are dimensioned in order to account for the data error bars.

to the N_2/NO_x flux, since this time range was found to be longer than the characteristic saturation time for the (RuPc) $_2$ thin films in these working conditions (gas flux, room temperature, and pressure). The sequences reported are immediately readable and can be easily interpreted despite consisting of raw spectra: A first piece of evidence is that, since the oscillation period is inversely proportional to film thickness, as the exposure continues, the film becomes thicker and thicker. Indeed, a progressive compression of the curves in Fig. 2 towards low q values can be followed by the naked eye till a certain time. Compression then stops, indicating that the sensing film is saturated with NO_x and that the thickness no longer changes. This kind of preliminary observation, i.e., the general features of the reaction kinetics, gives a qualitative indication on the overall morphological behavior. Indeed, the thickness versus exposure time curve will describe a trend consistent with this observation, so that possible artifacts can be easily revealed.

The resulting real-time evolution of the thickness parameter is reported in detail in Fig. 3(a). The values of the initial and final data points of the curves are precisely the information that can be deduced by the *ex situ* analysis, as discussed above. Instead, the real-time evolution of the thickness parameter is peculiar to the *in situ* x-ray reflectometry investigations.

As expected considering the preliminary overview of the raw pattern sequences in Fig. 2 two trends can be observed, which are separated by a crossover value, defined as d^* . Two different symbols are used in the graph to distinguish such different behaviors. Corresponding to the transition from the

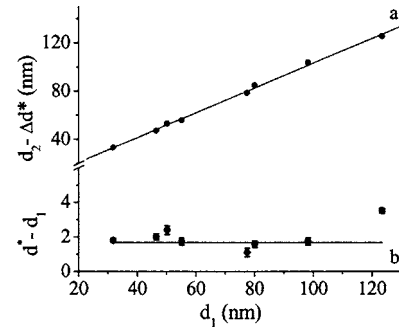


FIG. 4. The evolution of the different reaction stages as a function of the initial thickness is reported for a selection of samples: (a) second step thickness expansion, i.e., proportional increase, and (b) first step contribution only, i.e., constant increase; the error bars are estimated as the uncertainty in the d^* determination.

first to the second trend, i.e., at d^* , a sudden change in the slope of the curve can be seen. The visibility of the crossover can be enhanced by calculating the $d(t)$ curve derivative [Fig. 3(b)]. This twofold behavior was exhibited by all the (RuPc) $_2$ films studied, as shown in Figs. 3(c)–3(e), where a selection of the $d(t)$ curves is plotted.

The next step was to analyze the relevant parameters of each $d(t)$ curve separately. In Fig. 4(a) we report the $\Delta d^* = (d^* - d_1)$ values as a function of d_1 , while in Fig. 4(b) the $(d_2 - \Delta d^*)$ curve is plotted as a function of d_1 .

The first part of the whole thickness increase (Δd^*) is a constant, namely, is independent of d_1 . It can be fitted by the equation: $\Delta d^* = 1.68$ which is exactly the same value as the intercept of the linear function fitting the overall process. Moreover, the second part of the thickness increase ($d_2 - \Delta d^*$) can be fitted by the following equation:

$$(d_2 - \Delta d^*) = (1.027 \pm 0.02)d_1 + (0.43 \pm 0.30),$$

which is a linear function with the same slope as that related to the whole process and, within the uncertainty given by the determination of d^* , crossing the axis origin.

The conclusion that the hypothesis made on the basis of the *ex situ* data can be confirmed by analyzing time-resolved *in situ* data. Indeed, the latter allows the two distinct processes that take place upon exposure of the (RuPc) $_2$ sensing film to the NO_x flux to be distinguished.

A further confirmation to the two-step model can be obtained by using the same measurements to calculate the other morphological parameters detected by x-ray reflection, namely, the film surface roughness σ . Two σ vs t curves are shown in Fig. 5. In comparison with the corresponding d vs t curves, it can be noticed that exactly at the time when crossover occurs for the latter, the former also change their slopes. Of particular interest is the fact that the initial linear increase of $\sigma(t)$ is followed by an almost flat profile. This is fully consistent with the proposed model since it hypothesizes an increase of the surface roughness below t^* and is relative to the thickness crossover value d^* . This corresponds to the conclusion of the surface process, no further change of σ being expected above t^* .

Once the bulk process is also concluded, the (RuPc) $_2$ thin films do not desorb and the parameters d and σ remain constant, even if the samples are exposed to a N_2 flux, in our

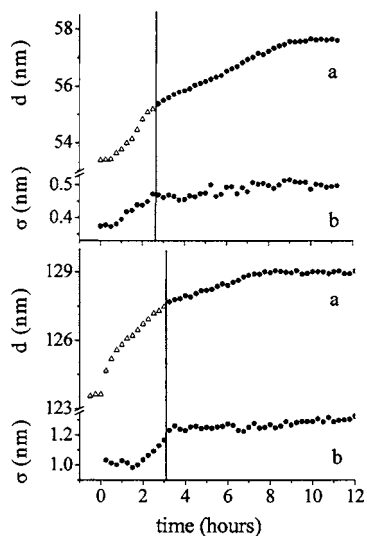


FIG. 5. The kinetic time evolution of thickness (a) and roughness (b) is shown for two different samples: (1) 52-nm-thick film and (2) 123-nm-thick film. In both cases there is a straightforward correlation between the two-step thickness evolution and the roughness.

case (180 nm/s). Moreover, no interaction with air is detectable, even after a number of weeks. This means that the $(\text{RuPc})_2$ thin film is stable at room-temperature and ambient pressure conditions, and their reflectivity spectra are reproduced perfectly, i.e., d_2 remains unchanged.

IV. CONCLUSIONS

In conclusion, with the time-resolved EDXR it is possible to observe a twofold reaction mechanism between $(\text{RuPc})_2$ and the active gas. This is unlikely in the one-step diffusion mechanism attributed to the other MePc, which is usually studied. The first step can be related to a surface mechanism with a negligibly small (or no) induction time; the second, is a diffusion process involving the film bulk.

This is consistent with the fact that the packing of the $(\text{RuPc})_2$ thin film is very different from the other MePc, frequently encountered in previous studies. However, determining the reason for the peculiar behavior of $(\text{RuPc})_2$ thin films upon exposure to NO_x gas is not possible on the basis of the EDXR data only. It is possibly due to the expansion of the film lattice induced by the penetration of gas molecules, or might involve more complex chemical reactions, such as the Ru- NO_x redox process. Therefore, further analysis, such as

photoemission spectroscopy or electric transport measurements, is still required in order to clarify whether the Ru metal, which is responsible for the structure and the packing of the films, also plays a role in the process of film swelling.

¹*Phthalocyanines: Properties and Applications*, edited by C. C. Leznoff and A. B. Lever (VCH, Cambridge, UK, 1989), Vols. 1–4.

²R. Dagani, *Chem. Eng. News* **74**(4), 22 (1996).

³*Phthalocyanines Materials, Synthesis, Structure and Function*, edited by N. B. Mckeown (Cambridge University Press, Cambridge, 1998).

⁴C. Hamann, A. Mrwa, M. Müller, W. Göpel, and M. Rager, *Sens. Actuators B* **4**, 73 (1991).

⁵J. Souto, R. De Aroca, and J. A. Saja, *J. Phys. Chem.* **98**, 8998 (1994).

⁶W. H. Ko, C. W. Fu, H. Y. Wang, D. A. Batzel, M. E. Kenney, and J. B. Lando, *Sens. Mater.* **2**, 39 (1990).

⁷A. Capobianchi, A. M. Paoletti, G. Pennesi, G. Rossi, and S. Panero, *Synth. Met.* **75**, 37 (1995).

⁸F. Baldini, A. Capobianchi, A. Falai, and G. Pennesi, *Sens. Actuators B* **51**, 176 (1998).

⁹C. Ercolani, A. M. Paoletti, G. Pennesi, G. Rossi, A. Chiesi-Villa, and C. Rizzoli, *J. Chem. Soc. Dalton Trans.* **1990**, 1971.

¹⁰A. Capobianchi, A. M. Paoletti, G. Pennesi, G. Rossi, R. Caminiti, and C. Ercolani, *Inorg. Chem.* **33**, 4635 (1994).

¹¹A. Generosi, V. Rossi Albertini, G. Rossi, G. Pennesi, and R. Caminiti, *J. Phys. Chem. B* **107**, 575 (2003).

¹²V. Rossi Albertini, A. Generosi, B. Paci, P. Perfetti, G. Rossi, A. Capobianchi, A. M. Paoletti, and R. Caminiti, *Appl. Phys. Lett.* **82**, 3868 (2003).

¹³H.-Y. Wang, C. W. Chiang, and J. B. Lando, *Thin Solid Films* **273**, 90 (1996).

¹⁴C. J. Liu, J. C. Hsieh, and Y. H. Ju, *J. Vac. Sci. Technol. A* **14**, 753 (1996).

¹⁵H. Y. Wang and J. B. Lando, *Langmuir* **10**, 790 (1994).

¹⁶A. T. J. Perr, A. Krier, and R. A. Collins, *Thin Solid Films* **273**, 90 (1996).

¹⁷Y. H. Ju, J. C. Hsieh, and C. J. Liu, *Thin Solid Films* **342**, 238 (1999).

¹⁸R. Caminiti, A. Capobianchi, P. Marovino, A. M. Paoletti, G. Pennesi, and G. Rossi, *Thin Solid Films* **382**, 74 (2001).

¹⁹K. Orita, T. Morimura, T. Horiuchi, and K. Matsushige, *Synth. Met.* **91**, 155 (1997).

²⁰X. L. Zhou and S. H. Chen, *Phys. Rep.* **257**, 223 (1995).

²¹S. K. Sinha, E. B. Sirota, S. Garoff, and H. B. Stanley, *Phys. Rev. B* **38**, 2297 (1988).

²²S. J. Roser, R. Felici, and A. Eaglesham, *Langmuir* **10**, 3853 (1994).

²³R. Caminiti and V. Rossi Albertini, *Int. Rev. Phys. Chem.* **18**, 263 (1999).

²⁴R. Felici, F. Cilloco, R. Caminiti, C. Sadun, and V. Rossi Albertini, Italy Patent No. RM 93 A000410 (1993).

²⁵L. G. Parratt, *Phys. Rev.* **95**, 359 (1954).

²⁶C. Teichert, J. F. MacKay, D. E. Savane, M. G. Lagally, M. Brohl, and P. Wagner, *Appl. Phys. Lett.* **66**, 2346 (1995).

²⁷Y. Samitsu, *Nanotechnology* **4**, 236 (1993).

²⁸A. Generosi, B. Paci, V. Rossi Albertini, P. Perfetti, G. Pennesi, A. M. Paoletti, G. Rossi, A. Capobianchi, and R. Caminiti, *Appl. Phys. Lett.* **86**, 114106 (2005).

²⁹J. C. Malaurent, H. Duval, J. P. Chauvineau, O. Hainaut, A. Raynal, and P. Dhez, *Opt. Commun.* **173**, 255 (2000).